



**Michigan
Technological
University**

Michigan Technological University
Digital Commons @ Michigan Tech

Dissertations, Master's Theses and Master's Reports

2016

EVALUATION OF ANGULAR DISTRIBUTION OF INCIDENT FIELD AT THE TRANSMISSION LOSS WINDOW IN MICHIGAN TECH'S REVERBERANT CHAMBER

Abhishek Thyagarajan
Michigan Technological University, thyagara@mtu.edu

Copyright 2016 Abhishek Thyagarajan

Recommended Citation

Thyagarajan, Abhishek, "EVALUATION OF ANGULAR DISTRIBUTION OF INCIDENT FIELD AT THE TRANSMISSION LOSS WINDOW IN MICHIGAN TECH'S REVERBERANT CHAMBER", Open Access Master's Report, Michigan Technological University, 2016.
<https://doi.org/10.37099/mtu.dc.etr/213>

Follow this and additional works at: <https://digitalcommons.mtu.edu/etr>



Part of the [Acoustics, Dynamics, and Controls Commons](#)

EVALUATION OF ANGULAR DISTRIBUTION OF INCIDENT FIELD AT THE
TRANSMISSION LOSS WINDOW IN MICHIGAN TECH'S REVERBERANT
CHAMBER

By

Abhishek Thyagarajan

A REPORT

Submitted in partial fulfillment of the requirements for the degree of

MASTER OF SCIENCE

In Mechanical Engineering

MICHIGAN TECHNOLOGICAL UNIVERSITY

2016

© 2016 Abhishek Thyagarajan

This report has been approved in partial fulfillment of the requirements for the Degree of MASTER OF SCIENCE in Mechanical Engineering.

Department of Mechanical Engineering – Engineering Mechanics

Report Advisor: *Andrew R. Barnard*

Committee Member: *Jason R. Blough*

Committee Member: *Charles D. Van Karsen*

Department Chair: *William W. Predebon*

Table of contents

1. Introduction	5
2. Theory	7
2.1 Transmission Loss	7
2.2 Transmission Loss test using the two room technique	9
2.3 Reverberation time	9
2.4 Diffuse field theory	10
2.5 Mass Law	11
2.6 Beamforming	11
2.7 Frequency domain beamforming	12
2.8 Beam pattern	13
2.9 Acoustic intensity	13
2.10 Phase calibration of intensity probe	14
3. Methods	15
3.1 Reverberation time	15
3.2 Beamforming	15
3.3 Acoustic intensity	17
4. Results	20
4.1 Reverberation time	20
4.2 Acoustic intensity results	20
4.3 Beamforming results	24
5. Conclusions	29
6. Future work	29
7. References	31
8. Appendix	33

List of figures

Figure 1: Random incidence(l) and field incidence(r)	6
Figure 2: TL curve and different regions of interest on the curve ⁴	8
Figure 3: Schematic representation of TL test using the two room method.....	9
Figure 4:Plane wave incident on an array ²⁰	12
Figure 5:Panel to mount array(l) and Location of reference microphone in the array(r)	16
Figure 6: Array mounted on the panel for test.....	16
Figure 7: Setup of acoustic intensity method	18
Figure 8: Acoustic intensity probe setup for all four axes of measurement; Clockwise from above (1) Horizontal axis (2) Vertical axis (3) Diagonal 1 axis (4) Diagonal 2 axis	19
Figure 9:Low frequency Intensity results for horizontal axis.....	20
Figure 10: High frequency Intensity results for horizontal axis	21
Figure 11: Low frequency Intensity results for vertical axis	21
Figure 12: High frequency Intensity results for vertical axis.....	22
Figure 13:Low frequency Intensity results for diagonal 1 axis	22
Figure 14: High frequency Intensity results for diagonal 1 axis.....	23
Figure 15: Low frequency Intensity results for diagonal 2 axis.....	23
Figure 16: High frequency Intensity results for diagonal 2 axis.....	24
Figure 17: Low frequency beamforming for horizontal axis.....	25
Figure 18:High frequency beamforming for horizontal axis.....	25
Figure 19: Low frequency beamforming for vertical axis	26
Figure 20:High frequency beamforming for vertical axis	26
Figure 21:Low frequency beamforming for diagonal 1 axis	27
Figure 22: High frequency beamforming for diagonal 1 axis.....	27
Figure 23:Low frequency beamforming for diagonal 2 axis	28
Figure 24:High frequency beamforming for diagonal 2 axis.....	28

Acknowledgment

I would like to thank my advisor, Dr. Barnard, for providing me the opportunity to work on this project and all the support he has provided to me over the last two years. I am grateful to him for being understanding through my delays and missteps through the course of this project and allowing me to find my way and arrive at the right place.

I also want to thank my parents, my family and Varsha for all their support, emotional and otherwise, through my graduate studies.

Abstract

Transmission Loss prediction accuracy is highly dependent on a good understanding of the angular distribution of incident field on the panel. Traditionally, the incident field has been assumed to be either completely random (equal probability of incidence at all angles from 0° - 90°) or field incidence (where the field is assumed to be completely diffuse between 0° - 78°). Studies¹⁻³ have shown that these models are not completely representative of the incident field. This incident field is studied in the Michigan Tech Transmission Loss suite using two different methods in this study; beamforming and acoustic intensity. The beamforming method uses a linear array and the acoustic intensity method uses an intensity probe mounted on a rotating platform that measures the incoming sound energy at different angles as it is swept over a range of angles. The results from these two methods show that the incident field approximately follows a $\cos^{0.8}(\theta)$ distribution.

1. Introduction

Transmission Loss (TL) is defined as the ratio of incident sound power to transmitted sound power through a barrier⁴. TL is an important metric used in automobile, aircraft and building industries to evaluate the acoustic performance of barriers and panels. Measurement of TL is a time consuming and involved process. This has incentivized development of analytical models that accurately predict TL of a panel based on its physical properties. Although there are models available that can predict TL to some accuracy, studies^{1,3} have shown that correlation between test TL and analytically estimated TL can be improved.

TL is measured by placing the specimen in an environment where there is a diffuse field on one side of the panel and the transmitted sound power is measured on the other side of the panel. A diffuse field is said to be present when there is spatial diffusion, where there is equal energy density at all points in the field and angular diffusion, where there is equal probability of energy incidence from all angles⁵. Although most well designed reverberant rooms may fulfil the first condition, the second condition is harder to meet⁶.

In analytical TL calculations, integration over a range of angles is considered to obtain an angle averaged TL¹. As explained previously, inducing a true angularly diffuse field is very difficult. This causes a deviation between analytical estimations of TL and measured TL. In

conventional calculations, the incident field is assumed to be either completely random (equal probability of incidence at all angles from 0° - 90°) or field incidence (where the field is assumed to be completely diffuse between 0° - 78°) where grazing incidence is not taken into account^{1,3,6}. These fields are illustrated in Figure 1.

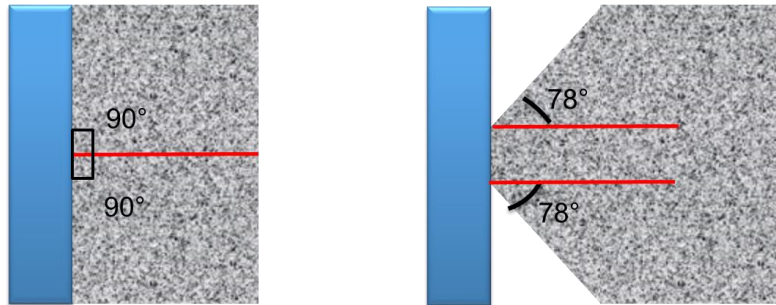


Figure 1: Random incidence(l) and field incidence(r)

Until recently, there were only a few studies that attempted to understand the angular distribution of reverberant field at the wall⁷⁻⁹. Kang^{1,2} and Lynch and Bauch³, recently have attempted to systematically study the incident field at the TL testing window. These studies indicate that rather than using uniform fields or field truncation, a model based on angle dependent sound field to be more appropriate. There have also been studies by Schiller¹⁰, Hasan¹¹, Nelisse¹² and others to study the sound field in the reverberant chamber using analytical and numerical methods. Schiller employs an analytical method and proposes a finite aperture correction that can be used to correct for the incident field¹⁰. Hasan uses numerical methods to study the spatial and angular distribution of energy in the reverberant room¹¹.

This study attempts to evaluate the incident field at the wall of the reverberant chamber using experimental methods. Previous studies using experimental methods to study the angular distribution of the incident field use two main techniques, beamforming^{3,13} and acoustic intensity^{1,3}. Kang¹ uses the acoustic intensity method to study the incident field. Lynch and Bauch³ uses both acoustic intensity and beamforming methods to study the incident field albeit at different test facilities. The beamforming method was performed at the Pennsylvania State University TL suite, also described in Bauch¹³, and the intensity method was performed at Gulfstream.

In Kang¹, the intensity probe was mounted in the aperture of the TL testing suite at the level of the panel. The source room was excited similar to when a TL test is performed¹⁴. The intensity probe was then rotated over a range of angles to obtain the intensity at each angle of incidence. This method is similar to the approach used by Lynch³ at Gulfstream. In the Penn State study, beamforming was performed by using two 41-point linear arrays to study the angular distribution of the incident field in both horizontal and vertical axes.

There is a discrepancy between the values predicted by the field incidence and random incidence models and the experimental results in all the studies. Kang¹ suggests a Gaussian distribution model for the diffuse field description while the model suggested by Lynch and Bauch³ is a $\cos^{1.2}(\theta)$. These models show a better correlation to the experimental results and show a 1 – 2 dB reduction in discrepancy when compared to the field incidence model.

Although the studies have empirically identified different models, they were all performed at different facilities using very different equipment and conditions. In order to determine which method of describing the incident field is most representative, the studies will need to be performed in the same facility under similar conditions.

The purpose of this study is to evaluate the two methods of incident field characterization in the same facility and under similar testing conditions to understand if there are any differences between the test methods and also evaluate relative merits of each method.

2. Theory

2.1 Transmission Loss

Transmission Loss is the ratio of sound power incident on a panel to the sound power transmitted through the panel. Transmission Loss is an important metric used to measure the effectiveness of a sound barrier. The relation for Transmission Loss is given by

$$TL = 10 \log_{10} \left(\frac{W_{incident}}{W_{transmitted}} \right) \quad (5)$$

where, $W_{incident}$ is the incident sound power on the panel or acoustic system and $W_{transmitted}$ is the sound power transmitted through the panel.

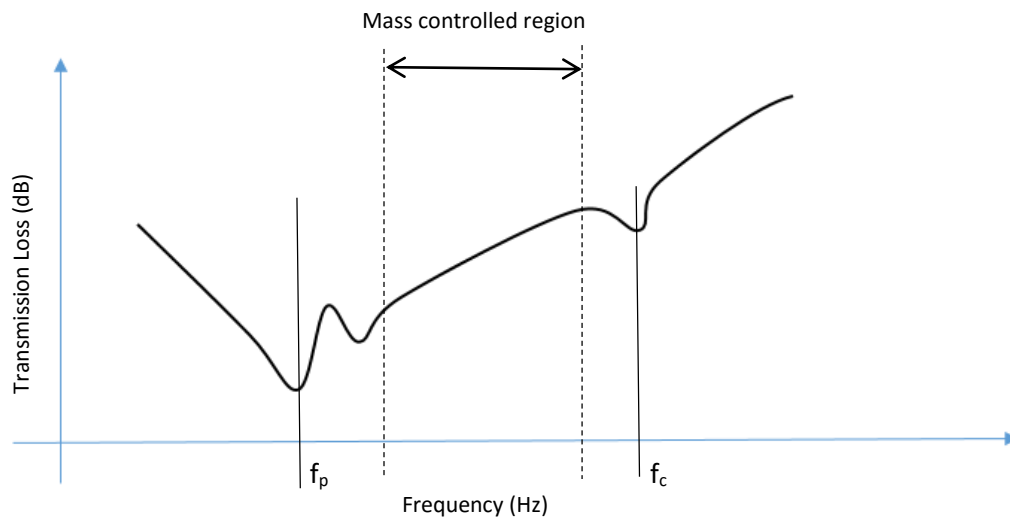


Figure 2: TL curve and different regions of interest on the curve⁴

Transmission Loss is a function of frequency and properties of the panel¹⁵. In low frequencies, TL is a function of the bending stiffness of the panel. At high frequencies, TL is a function of the damping and shear forces. The frequency below which bending stiffness dominates is called the fundamental panel mode (f_p). The frequency at which the wavenumber of the flexural vibration of the plate is equal to the wavenumber in the fluid is called coincident frequency (f_c)⁹. The region between fundamental panel mode and coincident frequency is the mass controlled region as shown in Figure 2. In this region, the panel behaves as a limp mass and its TL is only a function of its mass surface density. The TL in this region is given by the mass law described in the next section. This is a region of interest in many acoustic problems.

2.2 Transmission Loss test using the two room technique

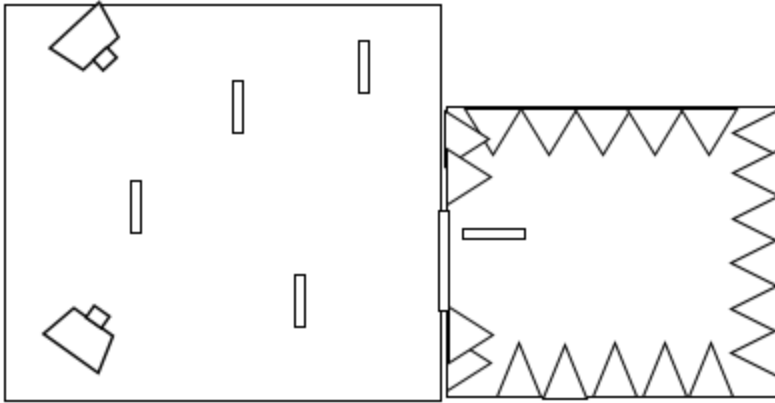


Figure 3: Schematic representation of TL test using the two room method

The two-room TL test using sound intensity is described in the ASTM E 2249 standard. In this test, the panel to be tested is mounted in an aperture between the reverberation and anechoic chambers as shown in Figure 3. The reverberation chamber is the source room where sound sources are placed in the corners to achieve a diffuse field. The reverberant field is sampled at various locations spatially and the spatially averaged sound pressure can be used to calculate the sound power of the sources as will be explained in the next section. The transmitted sound power is measured by measuring the surface averaged intensity of the panel as described in ASTM E 2249 and ISO 9614 -2¹⁶. The surface averaged sound intensity level and spatially averaged sound pressure levels can be used to compute the TL of the panel using the following relation

$$ITL = [L_1 - 6 + 10 \log_{10}(S_s)] - [\overline{L}_m + 10 \log_{10}(S_m)] \quad (1)$$

Where ITL is the Intensity Transmission Loss in dB, L_1 is the averaged sound pressure level in the source room in dB, S_s is the area of sample contained in measurement volume in m², \overline{L}_m is the surface averaged sound intensity of the panel in dB, S_m is the total area of the intensity measurement surface in m².

2.3 Reverberation time:

Reverberation time is an important characteristic of a reverberation chamber. This measure is important to understand as it affects the frequency ranges in which we can use the

reverberation chamber for acoustic measurements as will be explained in further sections. Reverberation time is the time taken by a sound to decay by 60 dB in a given room¹⁵. It is measured by exciting a room to a steady state, turning off the source and measuring the decay of the sound. Measurement of reverberation time of a room is described in ISO 3382¹⁷. It can also be estimated using equations like Sabine reverberation time relation. The Sabine definition of reverberation time is given as⁴,

$$T_{60} = \frac{0.161V}{A} \quad (2)$$

where, V is the volume of the room in cubic meters, The room absorption A is a product of $\bar{\alpha}$, the average surface absorption coefficient of the room and S , the total surface area of the room in squared meters. A is expressed as *Sabins*.

Understanding of the reverberant time is important in this case because the relation between sound pressure and sound power in a reverberant field is given by

$$L_w = L_p - 10 \log_{10} \left(\frac{4}{A} \right) \quad (3)$$

where L_p is the averaged sound pressure in dB re 20 μ Pa in the reverberant field and L_w is the sound power of the sources in dB re 1 pW.

2.4 Diffuse field theory

A diffuse field is said to be present in a room when the three following conditions are met⁵:

- 1) The energy density measured at all points in the room is the same
- 2) There is equal probability of energy incidence from all angles of incidence.
- 3) The phase relations between any two waves are random at every point in the room.

To achieve diffuse field, there should be sufficiently high modal density in the room to not have any distinct nodal or anti nodal points. At very low frequencies, when the wavelength is more than twice as long as any dimension of the room, the room behaves like a duct and only plane waves can propagate in it⁴. At slightly higher frequencies standing waves will propagate in the room with distinct nodal and anti-nodal points that are stationary. These standing waves occur at frequencies that are half integer multiples of any dimension of the room¹⁸. It is only at sufficiently high frequencies that the room will have sufficient modal

density to be diffuse. The theoretical frequency that divides the diffuse and non-diffuse field in a room is called the Schroeder frequency¹⁹. This is given by the following formula

$$f_s = 2000\sqrt{\frac{T}{V}} \quad (4)$$

where, T is the T_{60} time in seconds and V is the volume of the room in cubic meters. The Schroeder frequency is important to be noted in a reverberant chamber since it is considered to be the frequency above which the reverberant room is sufficiently diffuse and is the frequency above which measurements are considered in a reverberant chamber.

2.5 Mass Law

The mass law is an approximation of the transmission of a panel in the mass controlled region. In this region, the transmission coefficient is given by

$$\tau_\theta(\theta) = \left[1 + \left(\frac{\omega m_s \cos \theta}{2\rho_o c_o} \right)^2 \right]^{-1} \quad (6)$$

where τ_θ is the angle dependent transmission coefficient, ω is the angular frequency in radian/s, m_s is the surface mass density of the panel in kg/m², ρ_o is the density of the medium in kg/m³ and c_o is the speed of sound in the medium in m/s. The angle dependent TL is given by

$$TL = 10 \log_{10} \left(\frac{1}{\tau_\theta} \right) \quad (7)$$

2.6 Beamforming

Beamforming is a technique of spatial filtering where signals from a desired direction are amplified and those from undesirable directions are attenuated²⁰. It is used for directed transmission or reception of sound waves and also for sound imaging²¹. Beamforming can be performed in both time and frequency domains. It can be used to create a two or three dimensional image of the source. Similar to an intensity probe, the phase of the incoming wave is used to identify the angle of incidence in a linear array. The simplest beamformer is a

one dimensional array. The methods used in a one dimensional beamformer can be extended to two and three dimensional arrays²⁰.

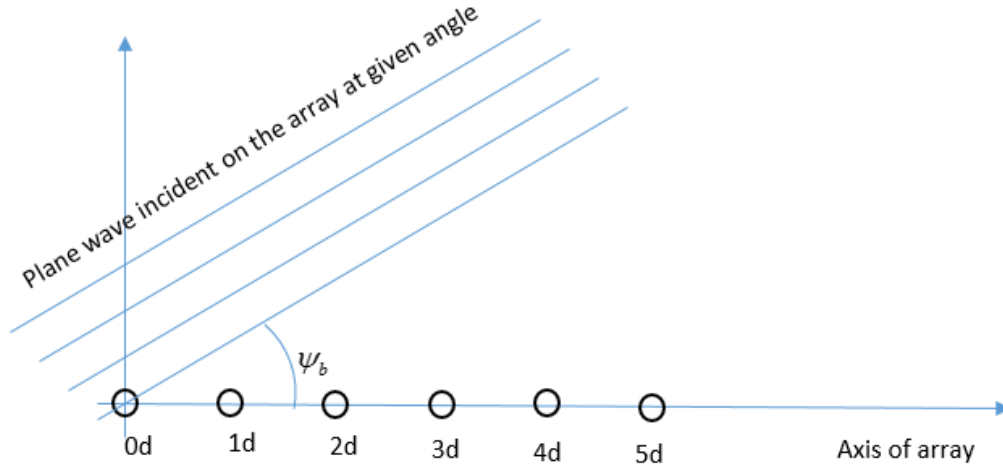


Figure 4: Plane wave incident on an array²⁰

Figure 4 shows a simple array on which a plane wave is incident. In this case, the time or phase delay between the reference microphone and any other microphone in the array will be a function of speed of sound, the distance between the microphone and the reference microphone and the angle of incidence of the sound wave. The time and phase delays between the microphones are important since this will be the one variable that will be used to spatially filter the incoming sound waves based on angle of incidence.

2.7 Frequency domain beamforming:

Frequency domain beamforming is the method used in this study as it allows us to study the diffusion characteristics of different frequencies. In this method, the beam is formed by applying a calculated phase shift to the signal at each sensor²⁰. This phase shift is given by

$$t_{mb} = m \frac{d}{c} \sin(\psi_b) \quad (8)$$

where, t_{mb} is the phase shift that is applied to the signal of each sensor, m is the m^{th} sensor in the array, d is the center - center distance between any two sensors in the array and ψ_b is the required beam steering angle.

The Fourier transform of the time signal is obtained and the phase shift is applied at every frequency bin. In addition to the speed of sound, distance from the reference microphone and steering angle of the beam, the weight in the weighted sum is also a function of frequency since phase difference between two microphones is affected by the wavelength. The steered beam is then given by¹³

$$P(\omega, \psi_b) = \sum_{m=0}^{M-1} H_m(\omega) e^{-j\omega r_{mb}} \quad (9)$$

where, P is the complex sound pressure in Pa, H_m is the frequency response function (frf) of the m^{th} microphone with the reference microphone and ω is the angular frequency in rad/s.

2.8 Beam pattern:

The beams that are obtained from the beamformer are inherently directional in nature since the signals received by the array elements vary with the direction of arrival²². The beam pattern has to be corrected for to ensure the obtained beam is an accurate representation of the sound pressures at the desired angle of incidence. The correction factor is given by

$$DI = \frac{M^2}{M + 2 \sum_{m=1}^{M-1} (M-m) \cos(2\pi m d u_o) \text{sinc}(2\pi d / \lambda)} \quad (10)$$

$$u_o = \frac{\sin(\psi_b) f}{c} \quad (11)$$

where, DI is the directivity index, M is the total number of sensors in the array, d is the center-center distance between sensors in the array, λ is the wavelength of the beam in m, f is the frequency in Hz and c is the speed of sound in m/s. The directivity factor is subtracted from the decibel value of the sound pressure level from the beamformer to obtain the corrected beam.

2.9 Acoustic Intensity:

Sound intensity or acoustic intensity is a measure of the amount of acoustic energy passing through a given area²³. Acoustic intensity can be used to identify the amount of sound energy that is flowing through a specific area at a specific angle. This is because intensity is a vector quantity whose direction is normal to that of the measurement area⁴.

$$W = IA \quad (12)$$

where, W is sound power in Watts, I is sound intensity in W/m^2 and A is area in m^2 .

Acoustic intensity is measured using intensity probes. There are two main types of intensity probes, p-p (pressure – pressure) intensity probes and p-u (pressure – velocity) intensity probes²⁴. In this study, p-p type of intensity probe is used to make all measurements. The pressure – pressure intensity probe uses a set of two phase matched microphones separated by a fixed distance to measure the pressure and the phase difference between the two microphones is used to calculate the intensity. The intensity from p-p probe is calculated using the following relation

$$I = \frac{\text{Im}(G_{12})}{\omega \rho \Delta r} \quad (13)$$

where, G_{12} is the cross spectrum between the two microphones in the intensity probe, $\text{Im}(G_{12})$ is the imaginary part of the cross spectrum, ω is the angular frequency in rad/s, ρ is the density of the medium in kg/m^3 and Δr is the distance between the two microphones in meters.

2.10 Phase calibration of intensity probe

The intensity measured by the probe is highly sensitive to the relative phase between the two microphones since the phase difference between the microphones is the value considered in calculating the intensity. The relative phases between the microphones hence have to be noted and corrected for to ensure accurate value of intensity is calculated. The phase mismatch calibration of the intensity probe is made by placing the microphones on two different openings on either side of the pistonphone and the cross spectrum between the microphones and auto spectra of each microphone is measured. The microphones are then switched and the same measurements are made again. The phase correction is then calculated as

$$G_{12}(\omega) = G'_{12}(\omega)e^{iC_{12}(\omega)/2} \quad (14)$$

$$C_{12} = \text{angle} \left(\frac{H_{12}}{H_{21}} \right) \quad (15)$$

where, H_{XY} is the Frequency Response Function (FRF) of microphone X with respect to microphone Y, G'_{12} is the uncorrected cross spectrum between microphones 1 and 2 and G_{12} is the corrected cross spectrum between the two microphones.

3. Methods

3.1 Reverberation time:

The reverberation time was measured using a Larson Davis Sound Level Meter (SLM). The reverberation chamber was excited to a steady state using a B&K sound source and the background levels were noted and the excitation levels were ensured to be 45 dB above background as per the ISO 3382:2008 standard¹⁷. The sound level meter was placed in the center of the room and the room was excited. When the source was shut off, the SLM measured the T20 and T30 times and calculated the T60 time of the reverberation chamber.

3.2 Beamforming:

Beamforming was performed to characterize the angular distribution of the incident sound field along the vertical, horizontal and diagonals of the TL window. The TL window at the Michigan Tech TL suite is 660 mm vertically and 673 mm horizontally. Four arrays were used to perform the TL study. The point at the center was used as the reference microphone since it was the common point for all arrays. The location of the reference point is shown in Figure 6. The horizontal and vertical arrays had 60 points each and the diagonals had 84 points each. Seven traversing and one reference ¼" PCB array microphones were used to collect the sound pressure time data. The phase references between each traversing microphone and the reference microphone was measured and corrected to ensure that the relative phase differences between the microphones was accounted for.

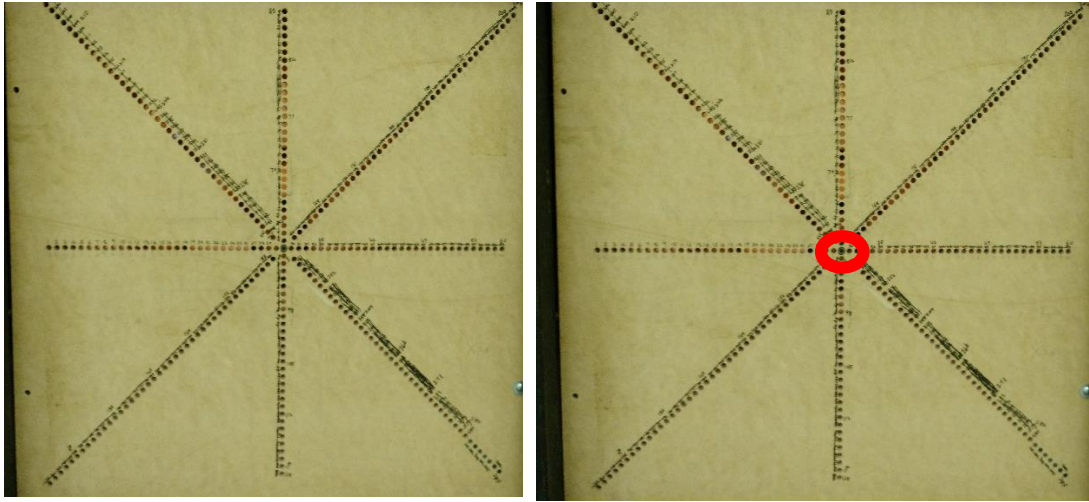


Figure 5: Panel to mount array(l) and Location of reference microphone in the array(r)

The center to center distance between each point on the array was 19.05 mm. The array was made on a $\frac{3}{4}$ " MDF panel mounted on the TL window as shown in Figure 7. The microphones were mounted flush on the array panel such that they did not intrude into the source room. Since the distances between the microphones was small, this could have affected the sound field being measured.

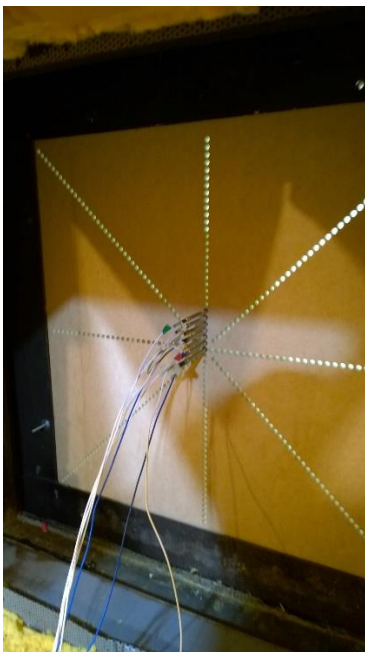


Figure 6: Array mounted on the panel for test.

The source room was energized using 3 sources. A B&K source was used along with 2 speakers placed in the corners. The room was excited using a broadband white noise between

300 – 10k Hz. The minimum frequency for which beamforming results were processed was 500 Hz. This was because the room is not diffuse below 500 Hz. This value was arrived at by performing the reverberation time test and computing the Schroeder frequency as explained previously. The Schroeder frequency of the room was estimated to be 504 Hz.

The cross spectra of each microphone with respect to the reference microphone and the auto spectra of the reference microphone was recorded for each set of data. A total of 42 sets of data were recorded for 288 array points. In this study, the absolute value at each point on the array is not important. What was of importance was to study the relative levels between each traversing microphone and the reference microphone. The FRF was computed from the auto spectra and cross spectra of the microphones. This ensured that the values obtained from different data sets could be used together. The data was sampled at 25600 Hz with a frequency resolution of 1 Hz. The data was averaged 120 times for each data set.

The data was then phase corrected in the same way that the intensity probe was phase calibrated. This phase corrected data from each data set was compiled and normalized to form the four arrays and the phase shift for each microphone was calculated based on the distance of the traversing microphone from the reference microphone²⁵. This phase shift is applied to each traversing microphone for all angles of incidence. The output from this is a matrix that has the complex sound pressures of each frequency for all angles of incidence from 0 – 180 degrees.

The output of the beamformer has to be corrected for directivity since the beam width changes as the beam is steered away from normal incidence. The output from the beamformer is normalized using the maximum incidence level at each frequency as reference. The output of the directivity index obtained from Equation 10 is a decibel value that is subtracted from the decibel output of the beamformer to obtain the corrected level for each frequency for incidence angles from 0° - 180° in 1° increments.

3.3 Acoustic intensity:

The acoustic intensity method was also used to characterize the angular diffusivity of the reverberation chamber. The intensity probe was fixed on a rotating platform such that the probe could be swept over a range of angles and the center of the probe was at the point at

which the panel would be present when mounted. The measurement was made at 37 different points from $0^\circ - 180^\circ$ in 5° increments.



Figure 7: Setup of acoustic intensity method

The mount was designed such that the intensity probe microphones would be at the center line horizontally, vertically and diagonal to the window. It was also made such that the probe did not intrude into the source room and the center point between the two microphones would not have an arc while the probe was swept through its range of motion. Figure 9 shown the setup for the intensity method.

The source room was excited in a similar way as during the beamforming method. The cross spectra of the two microphones were recorded for each angle increment and the sound intensity was computed for every 5° increment in angle of incidence. The intensity was then calculated using Equation 13. The measurements were made in all four axes; horizontal, vertical and two diagonals as shown in Figure 9.

The intensity measured by this method is then converted to third octave bands. The maximum value for each third octave band at each angle is used as reference to convert the One-Third Octave (OTO) intensity to decibels.

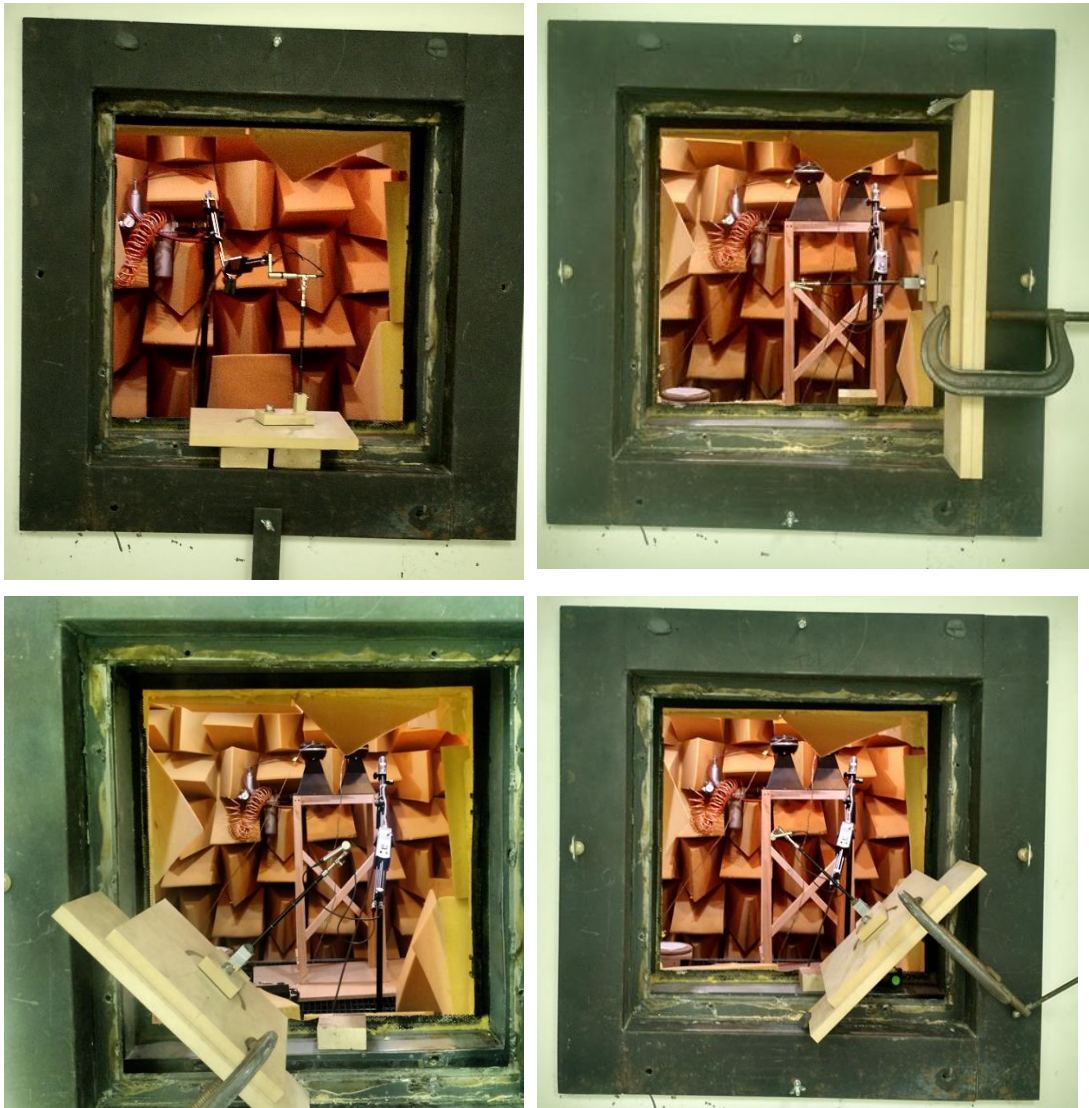


Figure 8: Acoustic intensity probe setup for all four axes of measurement; Clockwise from above (1) Horizontal axis (2) Vertical axis (3) Diagonal 1 axis (4) Diagonal 2 axis

4. Results

4.1 Reverberation time:

The measured T_{60} time for L_{eq} of white noise between 300 – 10000 Hz was 3.07s in the reverberation chamber and the volume of the reverberation chamber is 48.3345 cubic meters. From this, the Schroeder frequency of the reverberation room was calculated to be 504.8 Hz. It is because of this that the lowest OTO that is considered in this study is 500 Hz as the room is not diffuse below 500 Hz.

4.2 Intensity method:

Figures 9 - 16 show the results from the intensity method of the angular distribution evaluation. Here, diagonal 1 refers to the diagonal passing the bottom left corner to the top right corner and diagonal 2 refers to the diagonal passing through top left corner to the bottom right corner. The results are for 500 Hz OTO to 5000 Hz OTO on to which the $\cos^{0.8}(\theta)$ function is plotted. The results plotted are sound intensity level in dB referenced to the maximum value of intensity in every OTO. The plots show that the maximum intensity is near the normal incidence angle.

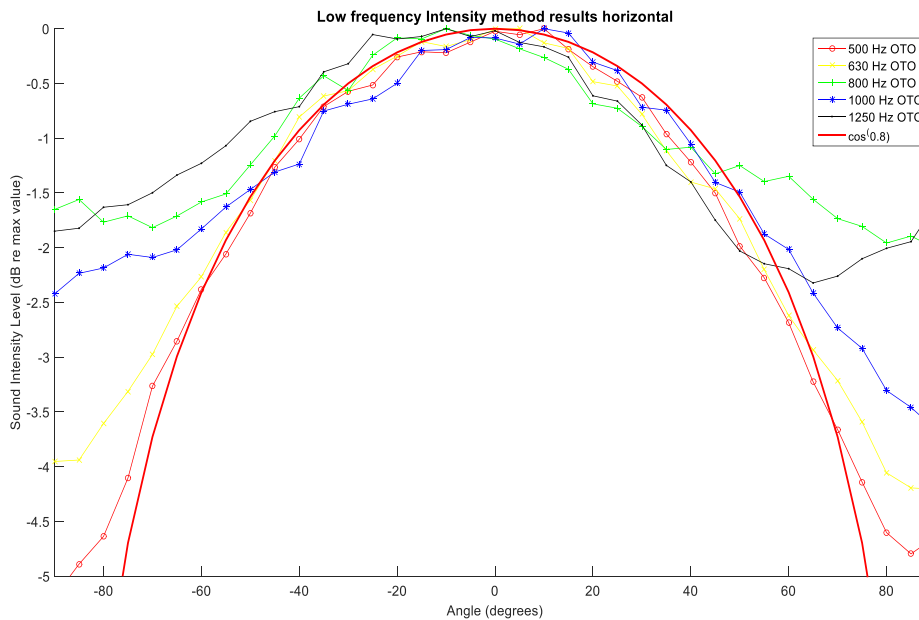


Figure 9: Low frequency Intensity results for horizontal axis

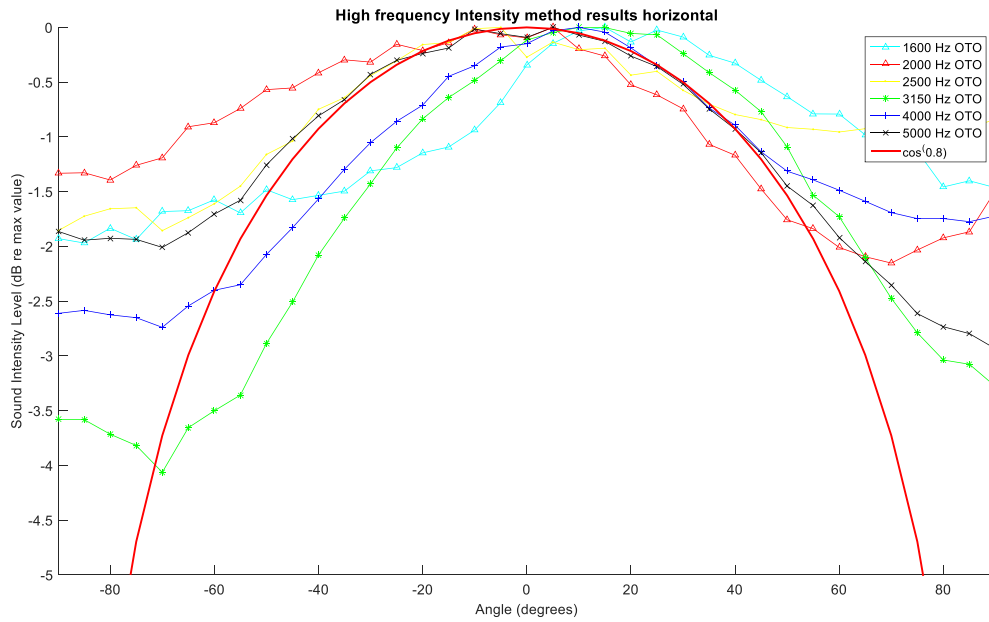


Figure 10: High frequency Intensity results for horizontal axis

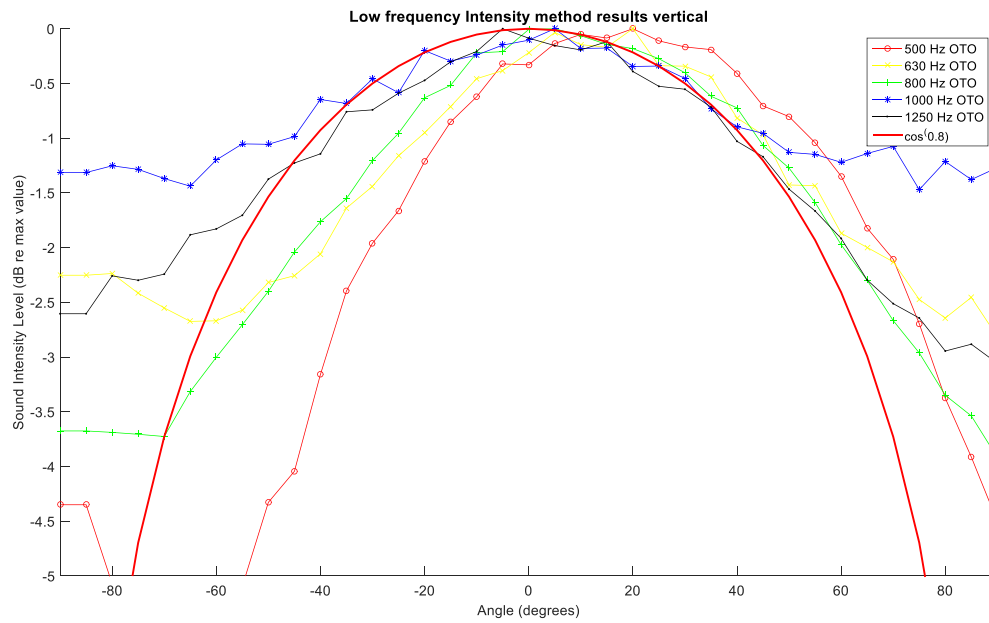


Figure 11: Low frequency Intensity results for vertical axis

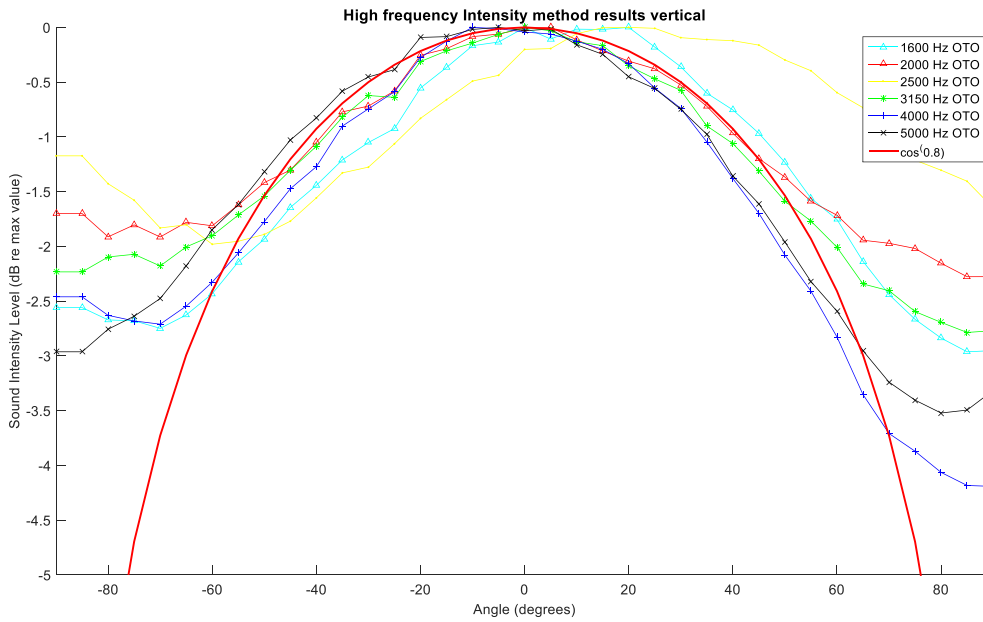


Figure 12: High frequency Intensity results for vertical axis

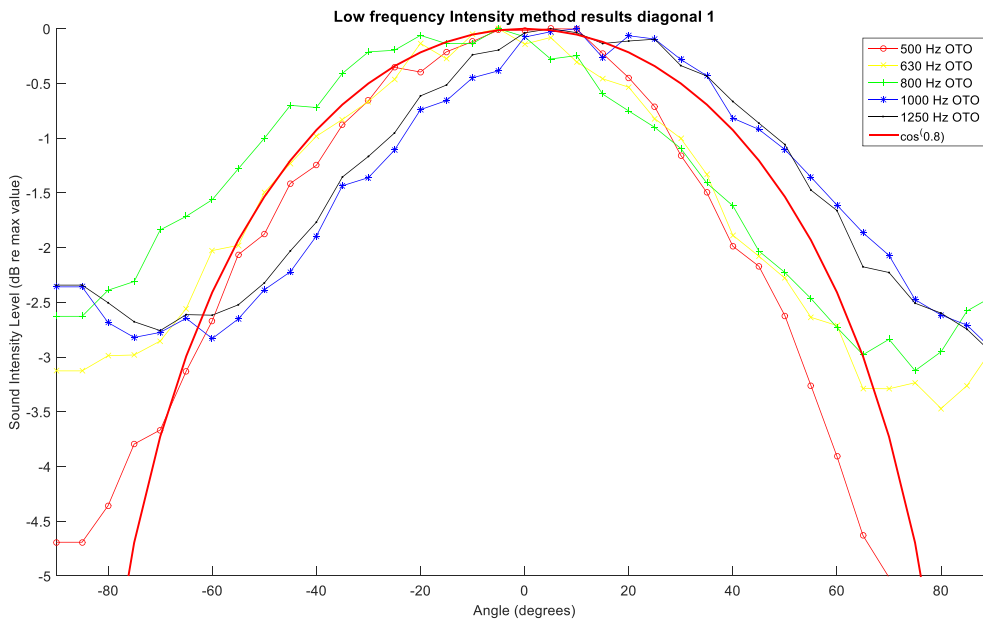


Figure 13: Low frequency Intensity results for diagonal 1 axis

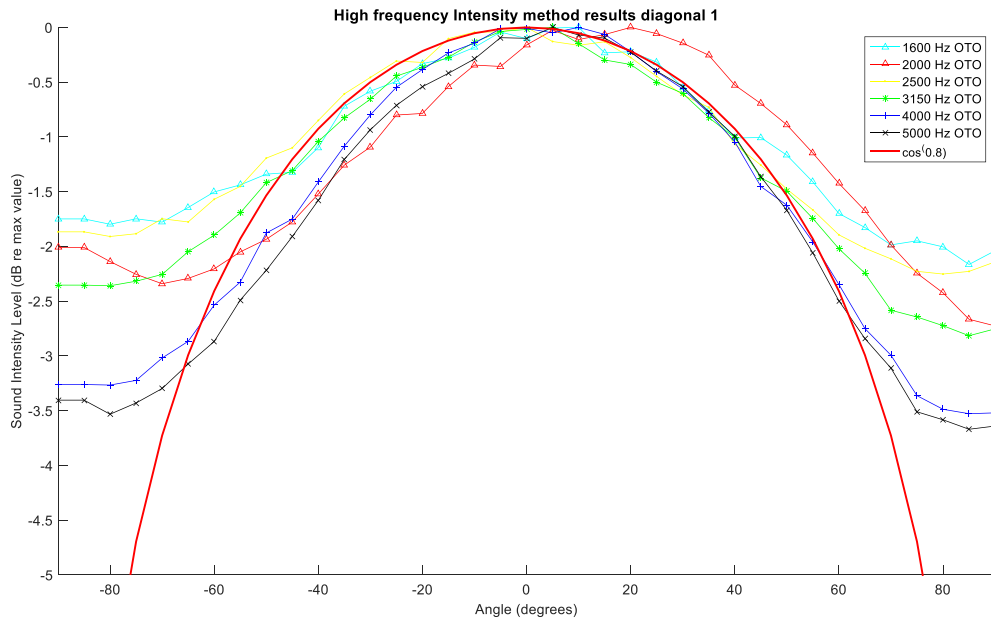


Figure 14: High frequency Intensity results for diagonal 1 axis

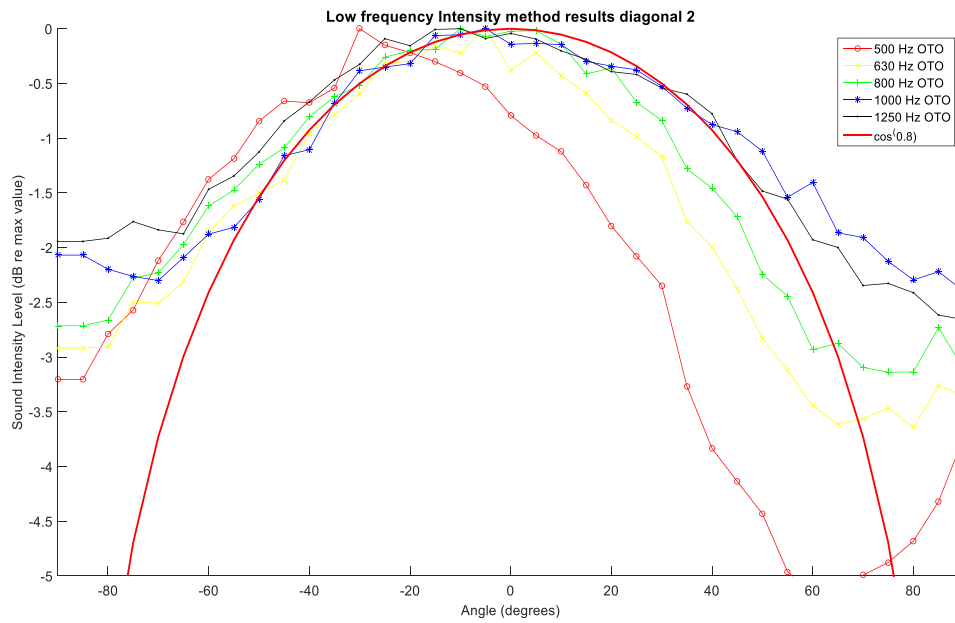


Figure 15: Low frequency Intensity results for diagonal 2 axis

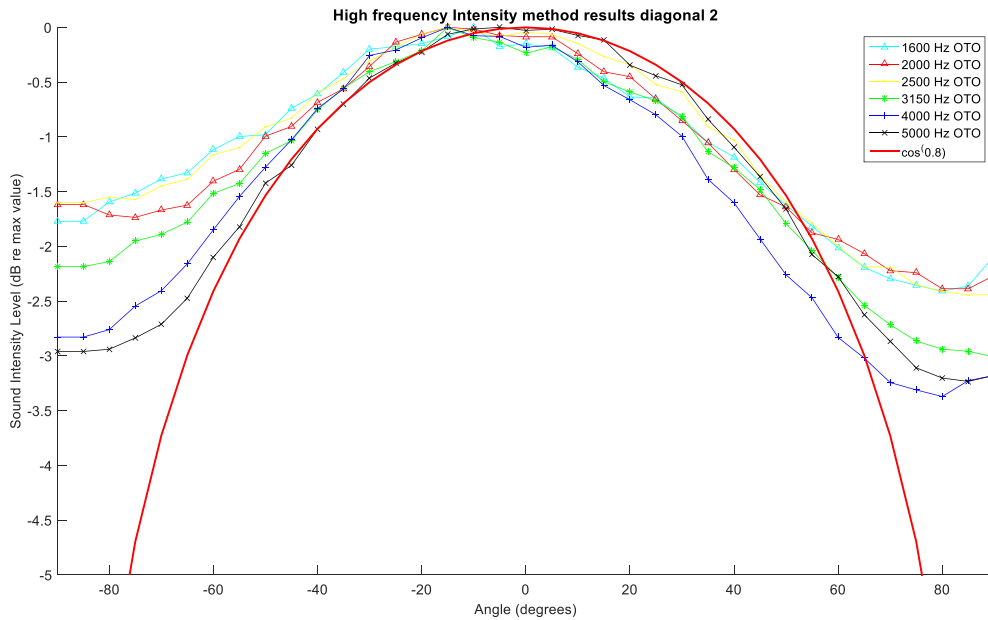


Figure 16: High frequency Intensity results for diagonal 2 axis

These results are similar to the beamforming results and they show that the range of sound intensity values are between 0 - 4 dB re max intensity. The $\cos^{0.8}(\theta)$ function agrees well with the angular distribution of incident energy.

4.3 Beamforming results:

The results from the beamforming method are shown in Figures 17 - 24 for all axes. The results shown below are for OTO from 500 Hz to 5000 Hz onto which the $\cos^{0.8}(\theta)$ function is plotted. The results are in decibel value of the sound pressure with reference to the maximum incident value in every OTO. The results as shown below, show that the variance in the sound pressure level over the range of angles on the panel is 0 - 5 dB re maximum incidence they are not absolute decibel values measured at the panel. The results also confirm that the maximum incidence in all cases is close to the normal incident angle.

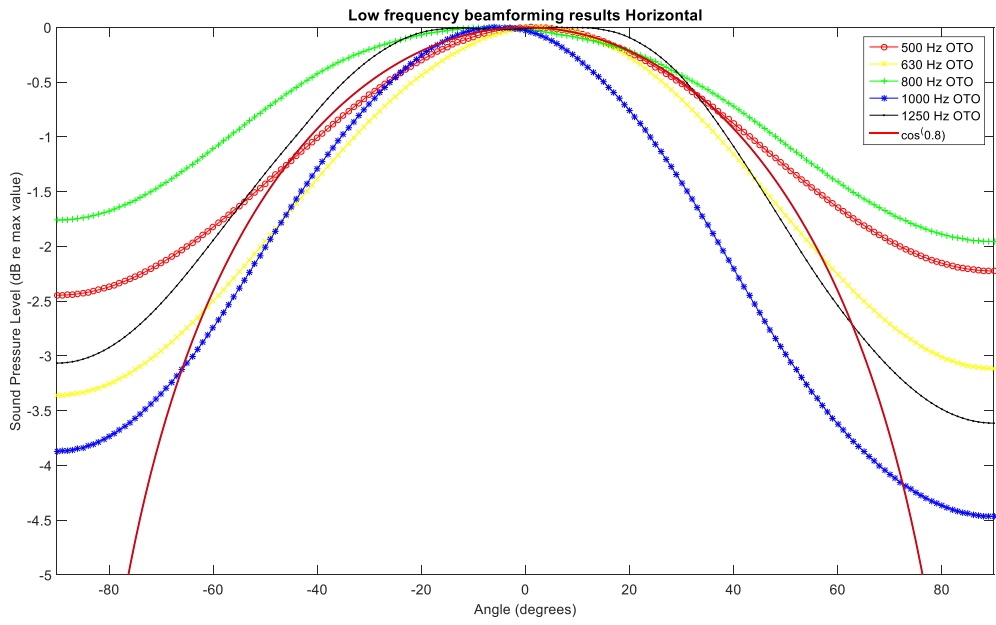


Figure 17: Low frequency beamforming for horizontal axis

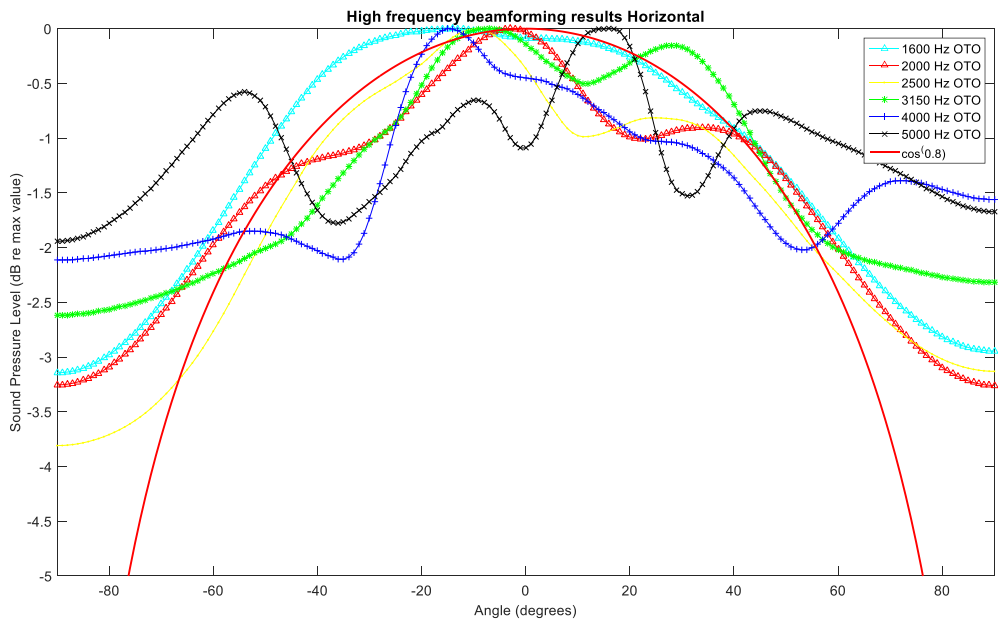


Figure 18: High frequency beamforming for horizontal axis

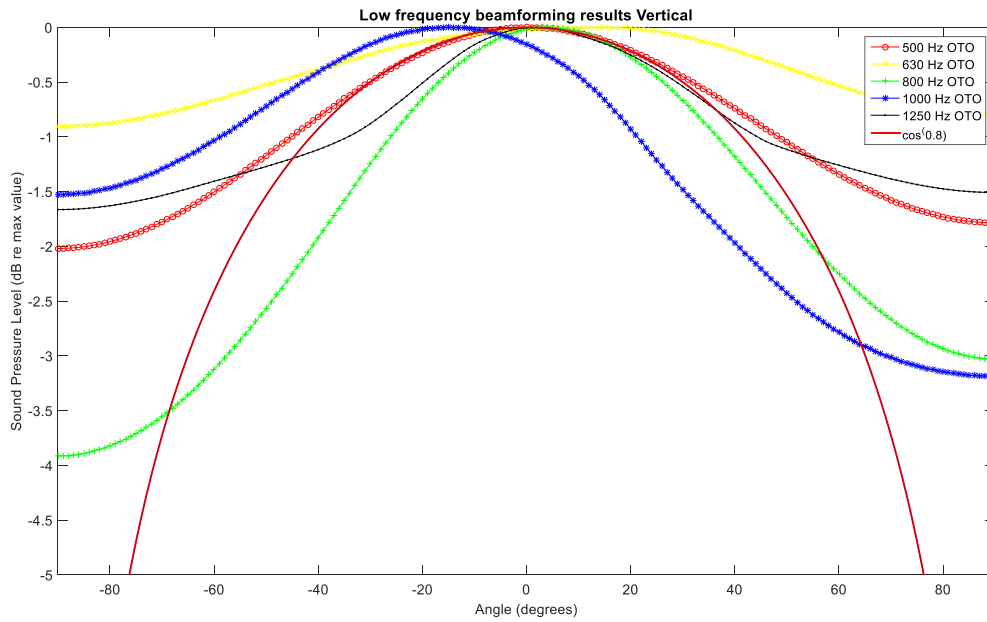


Figure 19: Low frequency beamforming for vertical axis

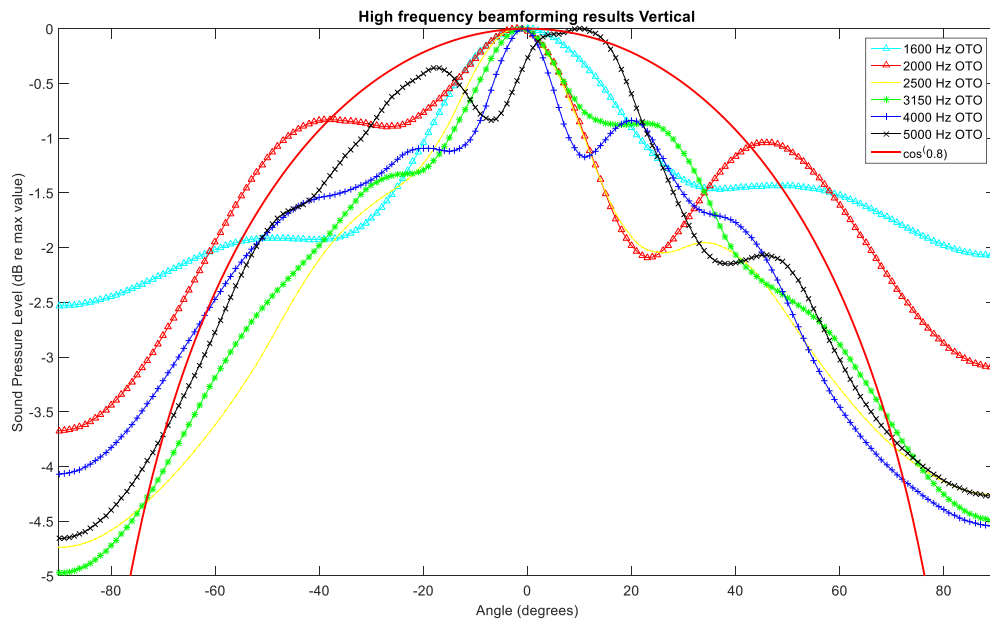


Figure 20: High frequency beamforming for vertical axis

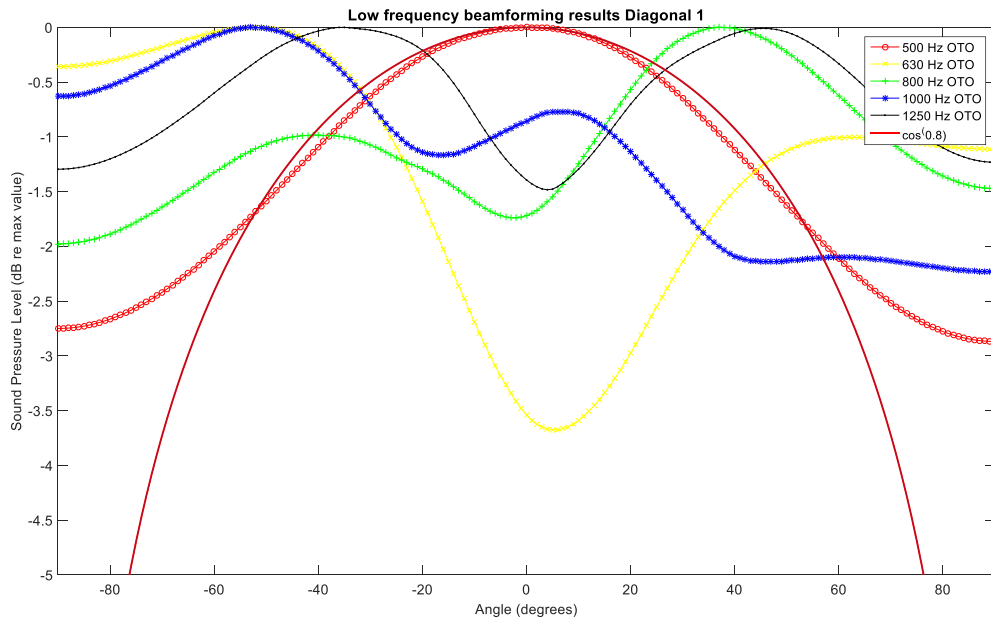


Figure 21: Low frequency beamforming for diagonal 1 axis

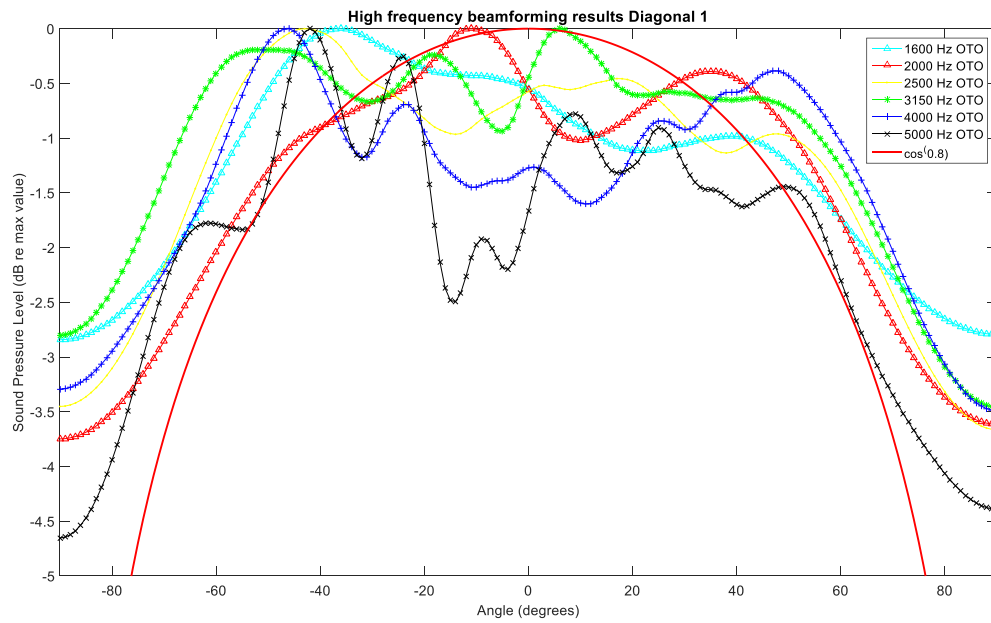


Figure 22: High frequency beamforming for diagonal 1 axis

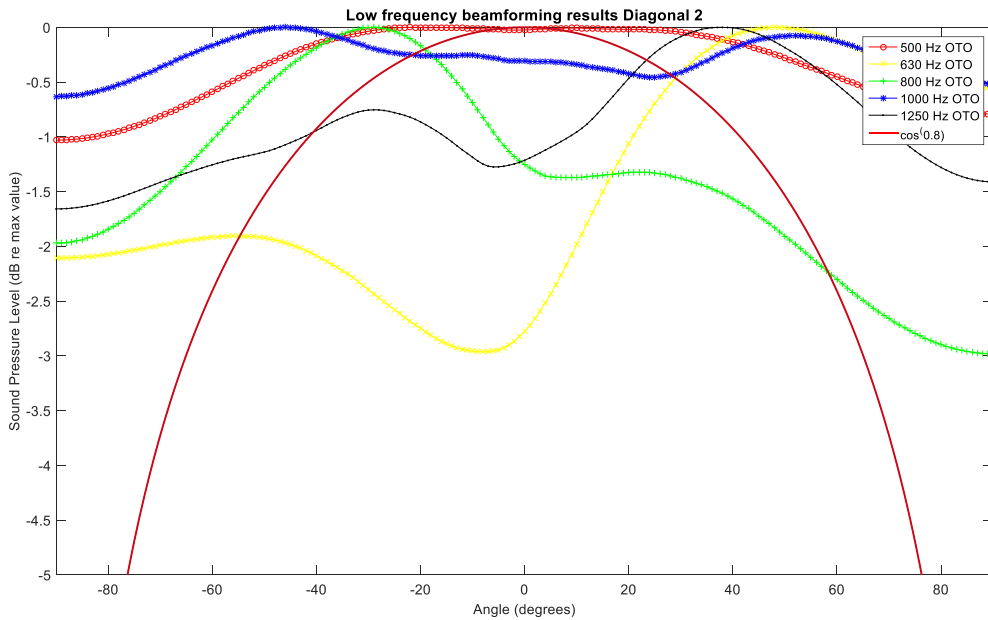


Figure 23: Low frequency beamforming for diagonal 2 axis

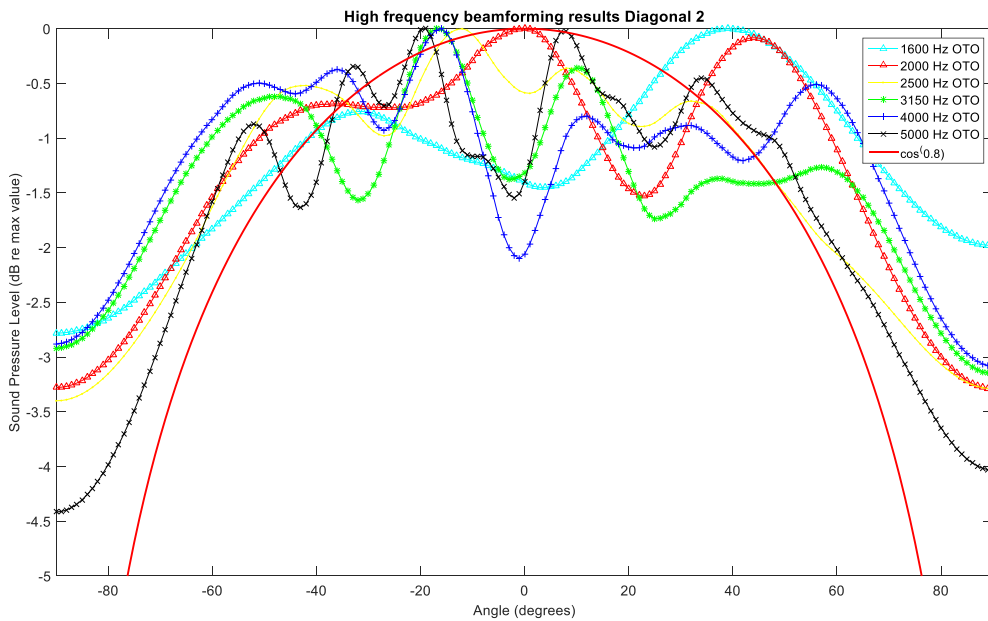


Figure 24: High frequency beamforming for diagonal 2 axis

There are some interesting findings from the above plots. The high frequency results seem less diffuse than the low frequency results and this is noteworthy since theoretically, higher

frequencies would be expected to be more diffuse than lower frequencies. Also, the correction factor $\cos^{0.8}(\theta)$ does not appear to fit the beamforming results as much as the intensity results. The difference between the two experimental results might explain the differences in the results. While the intensity probe was placed in the center of the window, away from any corners or edges, the beamformer had microphones that went up to the corner of the panel. There was also the array mounting panel present in the window while the beamforming measurements were made.

5. Conclusions

From the results, it can be seen that the angular distribution of incident energy cannot be described either by random incidence or a field truncated incidence model. In the Michigan Tech reverberant chamber, the $\cos^{0.8}(\theta)$ function is seen to describe the incident field for certain OTO in the intensity method. The results from the beamforming method do not describe the incident field in a way that is consistent between different OTO and different axes.

As indicated previously, the intensity and beamforming methods have not been performed in the same location under similar conditions. The results show that the distributions obtained by analyzing the field using the two methods are different and there is also some difference in the distribution based on the OTO under study. Based on these findings, rather than using one distribution model for all frequencies, different models might have to be used based on the OTO and also the method of incident field evaluation.

6. Future work

A TL study should be performed in the Michigan Tech TL suite and the correction factors obtained from both the methods can be used to compare with the measured TL and the relative accuracies can be compared.

Round robin tests between different test facilities should be done for both methods and TL of the same sample should be measured at both locations. Using the correction factors obtained using both methods, the accuracy of each method can be compared to the other.

The beamforming results show a sinusoidal variation of incident field at higher frequencies. This could be because the panel on which the microphones are mounted is excited by the sound field and has modes at these frequencies. These modes, when coupled with the

microphones could affect the beamforming results. This is because the beamforming results are highly sensitive to relative phases between microphones. When the array mounting panel is undergoing modes, the microphones might not all be on the same plane as to the reference microphone, causing phase relations that occur based on these modes rather than the direction of incident sound energy. This effect can be studied by performing the beamforming study with a setup that does not contain the panel. Understanding the effect panel modes have on the beamforming results will inform further designs of array mounts for beamforming studies.

7. References

1. H.-J.Kang J-GI, H.-S. Kim, J. -S. Kim. An experimental investigation on the directional distribution of incident energy for the prediction of sound transmission loss. *Applied Acoustics* 2002;63 (2002) 283–294.
2. Kang H-J, Ih J-G, Kim J-S, Kim H-S. Prediction of sound transmission loss through multilayered panels by using Gaussian distribution of directional incident energy. *The Journal of the Acoustical Society of America* 2000;107(3):1413-1420.
3. Kristopher Lynch PB, Stephen Hambric, Andrew Barnard. A proposed correction for incident sound intensity distribution for diffuse field panel excitation and transmission loss simulations. *NOISE-CON 2014*. Fort Lauderdale, Florida 2014.
4. Long M. *Architectural Acoustics*. Elsevier Academic Press; 2006.
5. Schultz TJ. Diffusion in reverberation rooms. *Journal of Sound and Vibration* 1971;16(1):17-28.
6. Jeong C-H. A correction of random incidence absorption coefficients for the angular distribution of acoustic energy under measurement conditions. *The Journal of the Acoustical Society of America* 2009;125(4):2064-2071.
7. Makita Y, Hidaka T. Revision of the $\cos \theta$ Law of Oblique Incident Sound Energy and Modification of the Fundamental Formulations in Geometrical Acoustics in Accordance with the Revised Law. *Acustica* 1987;63(3):163 - 173.
8. Makita Y, Hidaka T. Comparison between Reverberant and Random Incident Sound Absorption Coefficients of a Homogeneous and Isotropic Sound Absorbing Porous Material - Experimental Examination of the Validity of the Revised $\cos \theta$ Law. *Acustica* 1988;66 214 - 220.
9. de Bruijn A. Influence of Diffusivity on the Transmission Loss of a Single-Leaf Wall. *The Journal of the Acoustical Society of America* 1970;47(3A):667-675.
10. Schiller NH, Allen AR. Assessment of analytical predictions for diffuse field sound transmission loss. *Inter Noise*. San Francisco, CA, USA 2015.
11. Hasan MM, Hodgson M. Reverberation-Room Measurement Assuming a Diffuse Sound Field: Reviewing Standards and Reality. 2015; San Fransisco, CA, USA.
12. Nélisse H, Nicolas J. Characterization of a diffuse field in a reverberant room. *The Journal of the Acoustical Society of America* 1997;101(6):3517-3524.
13. Bauch P. Traditional and Angle Dependent Characterization of Penn State's Panel Transmission Loss Suite: Pennsylvania State University; 2013.
14. International A. Standard Test Method for Laboratory Measurement of Airborne Sound Transmission Loss of Building Partitions and Elements. Volume E 902002.
15. Lawrence E. Kinsler ARF, Alan B. Coppens, James V. Sanders. *Fundamentals of Acoustics*. John Wiley & Sons; 1982.
16. ISO. Determination of sound power levels using acoustic intensity - Part 2:. Measurement by scanning. Volume 9614 -21996.
17. ISO. Measurement of room acoustic parameters - Part 2: Reverberation time in ordinary rooms. 2008.
18. Harold W. Lord, William S. Gatley, Harold A. Evensen. *Noise Control For Engineers*. McGraw Hill Book Company; 1980.

19. KHEZRI SMS, Pedram Jafari. The Schroeder Frequency of Furnished and Unfurnished Spaces. *Romanian Journal of Acoustics & Vibration* 2012;9(2):113.
20. Grant Hampson AP. *Simulation of Beamforming Techniques for the Linear Array of Transducers*. Monash University; 1995.
21. Nolan M, Fernandez-Grande E, Jeong C-H. Characterization of diffusivity based on spherical array processing. *Inter Noise*. San Francisco, CA, USA2015.
22. McCowan I. *Robust Speech Recognition using Microphone Arrays*. Australia: Queensland University of Technology; 2001.
23. Mohan D. Rao US. Sound intensity and its applications in noise control. VII International Congress on Experimental Mechanics. Volume II. Las Vegas, Nevada1992.
24. Fahy F. *Sound Intensity*. Spon EF, editor: Chapman & Hall; 1995.
25. DeMuth G. Frequency domain beamforming techniques. 1977 May 1977. p 713-715.

8. Appendix

Appendix A

Beamforming code

```
clear
clc
%close all
addpath('Data', 'Matlab_code');
tic
%% Initialize file names
% Initialize array with the individual test results to load the
% cross
% spectra

test_list=['Set01.mat'; 'Set02.mat';...
    'Set03.mat'; 'Set04.mat'; 'Set05.mat'; 'Set06.mat'; ...
    'Set07.mat'; 'Set08.mat'; 'Set09.mat'; 'Set10.mat';...
    'Set11.mat'; 'Set12.mat'; 'Set13.mat'; 'Set14.mat'; ...
    'Set15.mat'; 'Set16.mat'; 'Set17.mat'; 'Set18.mat';...
    'Set19.mat'; 'Set20.mat'; 'Set21.mat'; 'Set22.mat';...
    'Set23.mat'; 'Set24.mat'; 'Set25.mat'; 'Set26.mat'; ...
    'Set27.mat'; 'Set28.mat'; 'Set29.mat'; 'Set30.mat';...
    'Set31.mat'; 'Set32.mat'; 'Set33.mat'; 'Set34.mat';...
    'Set35.mat'; 'Set36.mat'; 'Set37.mat'; 'Set38.mat'; ...
    'Set39.mat'; 'Set40.mat'; 'Set41.mat'; 'Set42.mat'];

%% Distance of mic from reference

d=0.00925;

%% Read test data and populate the different X and Auto spectra

% Initialize the G variable to take in all the data in blocks
G=zeros(10000,8,42);
% G is a 3-d matrix with row=freq, col=x and auto spec for each
% data set z-dir=specific data set
% Put data in the G matrix from the test data
for i=1:42
    load(test_list(i,:));
    G(:,:,i)=Cspec(:,1:8);
    clear Cspec;
end

% Isolate only frequencies between 401 to 6000
G1=G(401:6000,,:);

% Isolate only the first 8 columns of the C spec data
% Col 1 = Autospec of ref Col 2:7 = Crossspec of ref with array mics
```

```

G2=G1(:,1:8,:);

% Isolate the auto and cross spectra from G2
Aspec=G2(:,1,:);
Aspec=squeeze(Aspec);

% Isolate the cross spectra from G2
Xspec=G2(:,2:8,:);

fprintf('\nCompleted populating G\n');

%% Phase calibration

load('C.mat');
Corr=exp((1j*C)./2);
Corr=Corr(401:6000,:);
for i=1:42
    XC(:,:,i)=Xspec(:,:,i).*Corr;
end

%% Normalize all Xspec wrt the Aspec of that measurement
for i=1:41
    for j=1:7
        Xspec_norm(:,j,i)=XC(:,j,i)./Aspec(:,i);
    end
end
Xspec_norm(:,1,42)=XC(:,1,42)./Aspec(:,42);
% Concatenate the normed X spec end to end i.e. create 2-d from 3-d
Xspec3=zeros(5600,288);
j=1;
for i=1:41
    Xspec3(:,j:j+6)=Xspec_norm(:,:,i);
    j=j+7;
end
% Xspec2= normalized Xspec
Xspec3(:,288)=Xspec_norm(:,1,42);

%% Isolate the different sections of the data

% Horizontal Xspecs
Xh1=Xspec3(:,1:30);
Xhr=Xspec3(:,31:60);

Xh(:,2:31)=Xh1;
Xh(:,32:61)=Xhr;
Xh(:,1)=1;

% Vertical Xspecs
Xvu=Xspec3(:,61:90);
%Xvu=fliplr(Xvu_int);
Xvl=Xspec3(:,91:120);
Xv(:,2:31)=Xvu;

```

```

Xv(:,32:61)=Xv1;
Xv(:,1)=1;

% Diagonal Xspecs
Xd11=Xspec3(:,121:162);
Xdu1=Xspec3(:,163:204);
Xdu2=Xspec3(:,205:246);
Xd12=Xspec3(:,247:288);
Xd1(:,2:43)=Xd11;
Xd1(:,44:85)=Xdu1;
Xd1(:,1)=1;

Xd2(:,2:43)=Xdu2;
Xd2(:,44:85)=Xd12;
Xd2(:,1)=1;

lf=401;
uf=6000;
df=1;
sigs=Xv;
num_mics=60;
toc
fprintf('\nInitiating beamforming\n');
[B, Bint, LpB, LpB1, dir, corr1, corr2,
re]=beamform5(lf,df,uf,num_mics, d, sigs);
save('Horizontal_results_05302016_vert.mat', 'B', 'LpB', 'LpB1',
'dir', 'corr1',...
'corr2', 're');
fprintf('\nComplete\n');
toc

```

Appendix B

Beamform5 function

```
function [B, Bint, LpB, LpB1, dir, corr1, corr2,
re]=beamform5(lf,df,uf,num_mics, d, sigs)
%% Enter the data about test setup

%Speed of sound
c=343.59;
%Enter number of microphones in horizontal axis
nh=num_mics;
%Enter spacing between the microphones in mm (center to center)
d=d;

%% Distance from reference
% Horizontal axis; right of reference
for i=1:30
    dfrh(i+1)=(31-i)*d;
end
% Horizontal axis; left of reference
for j=31:60
    dfrh(j+1)=(j-30)*d;
end

dfrh(1)=0;
% Vertical axis; above reference
for k=61:90
    dfrv(k-60+1)=(k-60)*d;
end
% Vertical axis; below reference
for l=91:120
    dfrv(l-60+1)=(l-90)*d;
end

dfrv(1)=0;
% Diagonal axis; above reference
for i=1:42
    dfrd1(i+1)=(43-i)*d;
end
% Diagonal axis; below reference
for j=43:84
    dfrd1(j+1)=(j-43)*d;
end

dfrd1(1)=0;

dfr=dfrv;
%% Beamforming
```

```

FRF2=sigs;
% Horizontal
angles=-90:90;
radians=angles.*(pi/180);
freqs=lf:df:uf;
w=(2*pi).*freqs;

xx=(uf-lf)/df;
xx=xx+1;
Bint=zeros(xx,181,(nh+1));
% Apply phase shifts and calculate the beamformed result
for i=1:xx
    for j=1:181
        for k=1:(nh+1)
            tnb=(dfr(k)/c)*sin(radians(j));
            Bint(i,j,k)=FRF2(i,k)*exp(-1j*w(i)*tnb);
        end
    end
end
fprintf('\nComplete populating B\n');
B=zeros(xx,181);
% Bint=abs(Bint);
for i=1:(nh+1)
    B(:,:)=B(:,:)+Bint(:,:,i);
end
B=abs(B);
fprintf('\nComplete squeezing B\n');

% Isolate the maximum beamformed value for each frequency

[re,ang]=max(B,[],1);

% Decibel of beamformed result re max at each frequency bin
for i=1:181
    for j=1:xx
        LpB(j,i)=20.*log10(B(j,i)./re(j));
    end
end
fprintf('\nCompleted LpB\n');
% Decibel of beamformed result re normal incidence at each frequency
bin
for i=1:181
    for j=1:xx

        LpB1(j,i)=20.*log10(B(j,i)./B(j,91));
    end
end
fprintf('\nCompleted LpB1\n');

%% Directivity index

```

```

for i=1:xx
    for j=1:181
        uo(i,j)=sin(radians(j))*freqs(i)/c;
    end
end

lamb=c./freqs;

for i=1:xx
    for j=1:181
        D_int=0;
        for k=1:(nh+1)
            D_int=D_int+(nh-
k)*cos(2*pi*k*d*uo(i,j))*sinc(2*k*d/lamb(i));
        end
        dirint(i,j)=D_int;
    end
end

dir=nh^2./(nh+2.*dirint);
corr2=LpB1-dir;
bf1=LpB;
bf2=LpB1;

```

Appendix C

Intensity method

```
clear
clc
close all
%% Read the data

test_points=['Intensity01.mat';'Intensity02.mat';
'Intensity03.mat';...
'Intensity04.mat'; 'Intensity05.mat'; 'Intensity06.mat';
'Intensity07.mat';...
'Intensity08.mat'; 'Intensity09.mat'; 'Intensity10.mat';
'Intensity11.mat';...
'Intensity12.mat'; 'Intensity13.mat'; 'Intensity14.mat';
'Intensity15.mat';...
'Intensity16.mat'; 'Intensity17.mat'; 'Intensity18.mat';
'Intensity19.mat';...
'Intensity20.mat'; 'Intensity21.mat'; 'Intensity22.mat';
'Intensity23.mat';...
'Intensity24.mat'; 'Intensity25.mat'; 'Intensity26.mat';
'Intensity27.mat';...
'Intensity28.mat'; 'Intensity29.mat'; 'Intensity30.mat';
'Intensity31.mat';...
'Intensity32.mat'; 'Intensity33.mat'; 'Intensity34.mat';
'Intensity35.mat';...
'Intensity36.mat'; 'Intensity37.mat'];

for i=1:37
    load(test_points(i,:));
    Xpwr(:,i)=Cspec(:,2);
end

%% Intensity
%  $I = \text{imag}(p1p2^*) / (2 * \omega * \rho * \text{deltar})$ 
rho=1.29;
deltar=0.012;
f=1:10000;
omega=transpose(2*pi*f);
Ximag=imag(Xpwr)*1i;
den=-1./(omega*rho*deltar);

% Intensity value for each angle
for i=1:37
    I(:,i)=Ximag(:,i)./den;
end

I=abs(I);

% Calculate the OTO value for Intensity method
for i=1:37
```

```

[TOB,I_TOB(:,i)]=BandFiltering(transpose(f),I(:,i),'xtype','freq','y
type','linear','octaveorder',3,'outtype','linear');
end

for i=1:27
    re(i)=max(I_TOB(i,:));
end
% Decibel values of Intensity re max value at each OTO
for i=1:27
    I_dB_TOB(i,:)=10*log10(I_TOB(i,:)./re(i));
end

angles=-90:5:90;
ang=(angles.*pi)./180;
dist=cos(ang).^0.8;
distdb=10*log10(dist./dist(19));

% Plot the OTO values
figure(1)
spec=['o' 'x' '+' '*' '.'];
plot_color=['r' 'y' 'g' 'b' 'k'];
angles=-90:5:90;
hold on
for i=1:5
    plot(angles, I_dB_TOB(i+13,:), 'color',
plot_color(i), 'Marker', spec(i));
end
plot(angles,distdb, 'color', 'r', 'LineWidth', 2);
title('Low frequency Intensity method results horizontal');
xlabel('Angle (degrees)', 'FontSize', 15);
ylabel('Sound Intensity Level (dB re max value)', 'FontSize', 15);
legend('500 Hz TOB', '630 Hz TOB', '800 Hz TOB', '1000 Hz OTO', '1250
Hz OTO', 'cos^(0.8)');
xlim([-90, 90]);
ylim([-5, 0]);

hold off
set(gca, 'FontSize', 15)
figure(2)
spec=['^' '^' '.' '*' '+' 'x' 'o'];
plot_color=['c' 'r' 'y' 'g' 'b' 'k' 'c'];
angles=-90:5:90;
hold on
for i=6:11
    plot(angles, I_dB_TOB(i+13,:), 'color', plot_color(i-
5), 'Marker', spec(i-5));
end
plot(angles,distdb, 'color', 'r', 'LineWidth', 2);
title('High frequency Intensity method results horizontal');
xlabel('Angle (degrees)', 'FontSize', 15);
ylabel('Sound Intensity Level (dB re max value)', 'FontSize', 15);
legend('1600 Hz OTO', '2000 Hz OTO', ...

```

```
    '2500 Hz OTO', '3150 Hz OTO', '4000 Hz OTO', '5000 Hz  
OTO', 'cos^(0.8)');  
xlim([-90,90]);  
ylim([-5,0]);  
  
hold off  
set(gca, 'FontSize',15)
```